

# Attitude estimation from polarimetric cameras

**Abstract—**

## I. INTRODUCTION

Adaptation of large-field cameras and lenses such as omnidirectional and fisheye lenses are very popular in robotic application, simply due to the provided large field of view (360-degree) and extended amount of visual information. Due to these unique properties, these cameras are applicable in a wide range of robotics application, to name a few, visual odometry [19], navigation [25], simultaneous localization and mapping (SLAM) [8], and tracking [9]. Although great amount of visual information can be extracted from an omnidirectional image, our attention in this article is on the segment that often is ignored or not used as navigational clue, sky. In outdoor application, sky region often covers a large segment of omnidirectional or fisheye images and contains information, which has not been exploited to their full extend yet.

Sun position, stars and sky patterns are hold as navigational cues for the past centuries. Indeed, before the discovery of magnetic compass, these natural cues were the solitary source of navigation used by our ancestors [2, 7]. Skylight polarized pattern that is created due to scattered sunlight, is recognized as a navigation tool of some insects [24, 10]. The studies show that some insects such as desert ants (*cataglyphis*), butterflies and dragonflies among others, are able to navigate through their paths, efficiently and robustly by using the polarized pattern of sky, despite their small brains [10, 24, 5].

Acknowledging the nature, numerous studies have been conducted on polarized skylight pattern [11, 4, 26, 23, 3, 1, 21, 13, 15, 22, 12, 5]. These studies, often used the polarized pattern to create a sort of compass and estimate the solar azimuth angle and mainly have been shared in optic filed. Estimating polarized patterns, however, have been a difficult and complex task. The primary studies report the use of several photodiodes [11, 4, 26, 23, 3], while later either multiple cameras [1, 21, 22] or manual rotating filter [13, 15, 12, 5] were used. As a consequence of difficult and troublesome setups, exploiting the advantages of polarized patterns in our environment have been very limited. An example refers to the lack of using polarized sensors in Unmanned Aerial Vehicle (UAV). However, recent introduction of division-of-focal-plane (DoFP) micropolarizer cameras has offered an alternative solution [17, 16, 14]. In such cameras a micropolarizer filter array, composed of a pixelated polarized filters oriented at different angles, is aligned with a detector array. Thus they can simultaneously acquire linear polarization information (i.e  $S_0, S_1, S_2$ ) or full

stokes parameters in one image capture. Such a camera with a fisheye lens is used in this research to exploit the polarized information of sky region for attitude estimation. The used camera and their adaptation for robotics application is latter explained in Sect. III.

In the remainder of this paper, Sect. II provides a brief introduction to polarization by scattering, Rayleigh model and explains how these information can be used for attitude estimation. Sect. ?? represents our model for attitude estimation. Experiments and implementation details are explained in Sect. ??, and finally discussion and conclusion is presented in Sect. ??.

## II. POLARIZED CUES USED FOR ATTITUDE ESTIMATION

### A. Rayleigh scattering model

The unpolarized sunlight passing through our atmosphere gets scattered by different particles within the atmosphere. Beside deviating the direction of propagate wave, this transition also changes the polarization state of the incident light. This transition can be explained using Rayleigh scattering model. Rayleigh scattering describes the scattering of light or any electromagnetic waves by particles much smaller than their transmission wavelength. Accordingly it assumes that scattering particles of the atmosphere are small, homogeneous particles much smaller than the wavelength of the sunlight. Despite its simplification and assumption, this model proved to be sufficient for describing skylight scattering and polarization patterns [18, 6].

The Rayleigh scattering model predicts that the unpolarized sunlight becomes linearly polarized passing through the atmosphere. Equation 1 shows the stokes vector for natural light after and before passing through the atmosphere, since the last stokes parameter is 0 after scattering, the light is considered to be linearly polarized.

$$s_{unp} = \begin{bmatrix} 1 \\ 0 \\ 0 \\ 0 \end{bmatrix} \xrightarrow{\text{scattering}} s_p = \begin{bmatrix} s_0 \\ s_1 \\ s_2 \\ 0 \end{bmatrix} \quad (1)$$

Having the stokes parameters the degree of linear polarization (DoPl) ( $\rho_l$ ) in terms of stokes parameters and the scattering angle ( $\gamma$ ), respectively is presented as:

$$\rho_l = \frac{\sqrt{s_1^2 + s_2^2}}{s_0} = \frac{\sin^2(\gamma)}{\cos^2(\gamma) + 1} \quad (2)$$

where scattering angle  $\gamma$  is the angular distance between the celestial point observed and the sun. According to Rayleigh model, the DoPl,  $\rho_l$ , varies from 0 to  $\approx 1$  depending on the scattering angle,  $\gamma$ , ( $\rho_l = 0$  while  $\gamma = 0, \pi$  and  $\rho_l \approx 1$  while

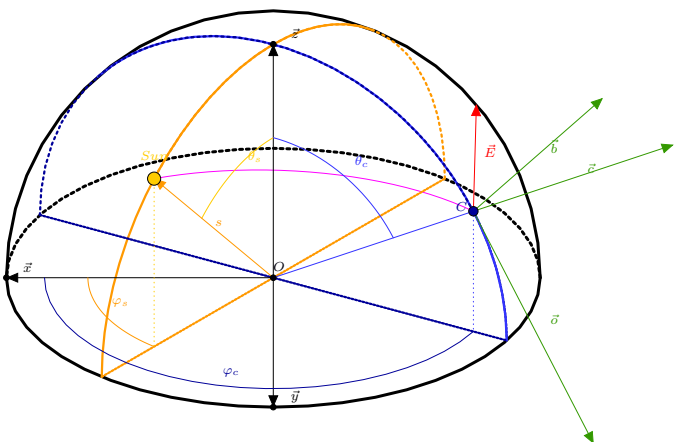


Fig. 1. Skylight polarization by scattering  
The figure needs to be re-designed according the text

$\gamma = \pi/2$ ) [20, 15]. Accounting for the approximation and polarization defect, Eq. 2 is presented as [18]:

$$\rho_l = \rho_{l_{max}} \frac{1 - \cos^2(\gamma)}{1 + \cos^2(\gamma)} \quad (3)$$

#### B. Polarization by scattering model for sky pattern

This section represent the relations between polarized measurements in pixel frame  $\mathcal{P}$  and sun and celestial point in the world frame  $\mathcal{W}$ .

Based on Rayleigh scattering the electric field of incident light after scattering is perpendicular to the scattering plane, that is defined by the observer, celestial point and the sun. This plane is highlighted by light shade of red in Fig. reffig:scattering and is represented by a sun vector  $\vec{s}$  and celestial vector  $\vec{c}$ .

Accordingly the normalized electric field vector  $\vec{E}$  in the world frame is presented as the normalized cross product of  $\vec{s}$  and  $\vec{c}$  (see Eq. 4).

$$\vec{E} = \frac{\vec{s} \wedge \vec{c}}{\|\vec{s} \wedge \vec{c}\|} \quad (4)$$

However measuring the skylight polarization pattern and angle of polarization (AoP), the electric field in the pixel frame  $\mathcal{P}$  ( $\widehat{obc}$ ) is represented as:

$$E_{obc} = \begin{bmatrix} E_o \\ E_b \\ 0 \end{bmatrix} = \begin{bmatrix} \cos \alpha \\ \sin \alpha \\ 0 \end{bmatrix} \quad (5)$$

where  $\alpha$  is the measured angle of polarization. Combination of equation (4) and (5) and using the scattering angle  $\gamma$ , between  $\vec{s}$  and  $\vec{c}$  leads to:

$$\begin{cases} (\vec{s} \wedge \vec{c}) \cdot o &= \sin \gamma \cos \alpha \\ (\vec{s} \wedge \vec{c}) \cdot b &= \sin \gamma \sin \alpha \end{cases}, \quad (6)$$

applying vector triplet cross product rule on Eq. 6 results.

$$\begin{cases} s \cdot b &= \sin \gamma \cos \alpha \\ s \cdot o &= -\sin \gamma \sin \alpha \end{cases} \quad (7)$$

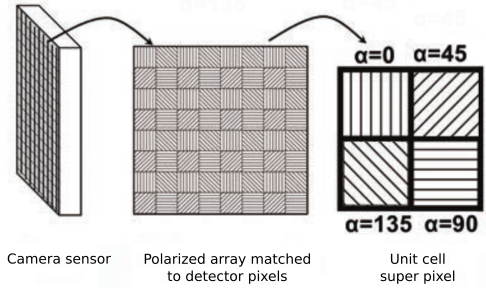


Fig. 2. Structure of DoFP sensors

Considering the DoPl (see Eq. ??), the scattering angle  $\gamma$ , therefore can be represented as:

$$\cos \gamma = s \cdot c = \pm \sqrt{\frac{1 - \rho'_l}{1 + \rho'_l}} \quad (8)$$

with  $\rho'_l = \frac{\rho_l}{\rho_{l_{max}}}$ .

Equations 7 and 8 finally leads to the sun vector in pixel frame  $\mathcal{P}$  which express a direct relation between the measured polarization parameters (AoP ( $\alpha$ ), DoPl ( $\rho$ )), scattering angle ( $\gamma$ ), the sun position, and the celestial point:

$$\vec{s}_{\mathcal{P}} = \begin{bmatrix} -\sin \gamma \sin \alpha \\ \sin \gamma \cos \alpha \\ \cos \gamma \end{bmatrix} \quad (9)$$

### III. SETTING THE POLARIMETRIC CAMERA FOR ROBOTICS

#### IV. ATTITUDE ESTIMATION

#### REFERENCES

- [1] J. R. Ashkanazy and J. Humbert, "Bio-inspired absolute heading sensing based on atmospheric scattering," in *AIAA Guidance, Navigation, and Control Conference*, 2015, p. 0095.
- [2] A. Barta, V. B. Meyer-Rochow, and G. Horváth, "Psychophysical study of the visual sun location in pictures of cloudy and twilight skies inspired by viking navigation," *JOSA A*, vol. 22, no. 6, pp. 1023–1034, 2005.
- [3] J. Chahl and A. Mizutani, "Integration and flight test of a biomimetic heading sensor," in *Proc. SPIE*, vol. 8686, 2013, p. 86860E.
- [4] J. Chu, H. Wang, W. Chen, and R. Li, "Application of a novel polarization sensor to mobile robot navigation," in *International Conference on Mechatronics and Automation. ICMA 2009*. IEEE, 2009, pp. 3763–3768.
- [5] M. Hamaoui, "Polarized skylight navigation," *Applied Optics*, vol. 56, no. 3, pp. B37–B46, 2017.
- [6] G. Horváth, A. Barta, J. Gal, B. Suhai, and O. Haiman, "Ground-based full-sky imaging polarimetry of rapidly changing skies and its use for polarimetric cloud detection," *Applied optics*, no. 3, pp. 543–559, 2002.
- [7] G. Horváth, A. Barta, I. Pomozi, B. Suhai, R. Hegedüs, S. Åkesson, B. Meyer-Rochow, and R. Wehner, "On the trail of vikings with polarized skylight: experimental study of the atmospheric optical prerequisites allowing polarimetric navigation by viking seafarers," *Philosophical Transactions of the Royal Society of London B: Biological Sciences*, vol. 366, no. 1565, pp. 772–782, 2011.
- [8] J.-H. Kim and M. J. Chung, "Slam with omni-directional stereo vision sensor," in *International Conference on Intelligent Robots and Systems*, 2003, vol. 1. IEEE, 2003, pp. 442–447.
- [9] M. Kobilarov, G. Sukhatme, J. Hyams, and P. Batavia, "People tracking and following with mobile robot using an omnidirectional camera and a laser," in *IEEE International Conference on Robotics and Automation, ICRA*. IEEE, 2006, pp. 557–562.

- [10] T. Labhart and E. P. Meyer, "Neural mechanisms in insect navigation: polarization compass and odometer," *Current opinion in neurobiology*, vol. 12, no. 6, pp. 707–714, 2002.
- [11] D. Lambrinos, R. Müller, T. Labhart, R. Pfeifer, and R. Wehner, "A mobile robot employing insect strategies for navigation," *Robotics and Autonomous Systems*, vol. 30, no. 12, pp. 39 – 64, 2000. [Online]. Available: <http://www.sciencedirect.com/science/article/pii/S0921889099000640>
- [12] H. Lu, K. Zhao, Z. You, and K. Huang, "Angle algorithm based on hough transform for imaging polarization navigation sensor," *Optics express*, vol. 23, no. 6, pp. 7248–7262, 2015.
- [13] T. Ma, X. Hu, L. Zhang, J. Lian, X. He, Y. Wang, and Z. Xian, "An evaluation of skylight polarization patterns for navigation," *Sensors*, vol. 15, no. 3, pp. 5895–5913, 2015.
- [14] J. Millerd, N. Brock, J. Hayes, M. North-Morris, B. Kimbrough, and J. Wyant, "Pixelated phase-mask dynamic interferometers," *Fringe 2005*, pp. 640–647, 2006.
- [15] D. Miyazaki, M. Ammar, R. Kawakami, and K. Ikeuchi, "Estimating sunlight polarization using fish-eye lens," in *IPSJ Transactions on Computer Vision and Applications*, vol. 1, 2009, pp. 288–300.
- [16] G. P. Nordin, J. T. Meier, P. C. Deguzman, and M. W. Jones, "Diffractive optical element for stokes vector measurement with a focal plane array," in *Proc. SPIE*, vol. 3754, 1999, pp. 169–177.
- [17] ———, "Micropolarizer array for infrared imaging polarimetry," *JOSA A*, vol. 16, no. 5, pp. 1168–1174, 1999.
- [18] I. Pomozi, G. Horvath, and R. Wehner, "How the clear-sky angle of polarization pattern continues underneath clouds: full-sky measurements and implications for animal orientation," *The Journal of Experimental Biology*, vol. 204, pp. 2933–2942, 2001.
- [19] D. Scaramuzza and R. Siegwart, "Appearance-guided monocular omnidirectional visual odometry for outdoor ground vehicles," *IEEE transactions on robotics*, vol. 24, no. 5, pp. 1015–1026, 2008.
- [20] G. S. Smith, "The polarization of skylight: An example from nature," *American Journal of Physics*, vol. 75, no. 1, pp. 25–35, 2007.
- [21] W. Stürzl and N. Carey, "A fisheye camera system for polarisation detection on uavs," in *European Conference on Computer Vision*. Springer, 2012, pp. 431–440.
- [22] D. Wang, H. Liang, H. Zhu, and S. Zhang, "A bionic camera-based polarization navigation sensor," *Sensors*, vol. 14, no. 7, pp. 13 006–13 023, 2014.
- [23] Y. Wang, J. Chu, R. Zhang, L. Wang, and Z. Wang, "A novel autonomous real-time position method based on polarized light and geomagnetic field," *Scientific reports*, vol. 5, 2015.
- [24] R. Wehner, "Desert ant navigation: how miniature brains solve complex tasks," *J Comp Physiol A*, vol. 189, pp. 579–588, 2003.
- [25] N. Winters, J. Gaspar, G. Lacey, and J. Santos-Victor, "Omnidirectional vision for robot navigation," in *IEEE Workshop on Omnidirectional Vision*. IEEE, 2000, pp. 21–28.
- [26] K. Zhao, J. Chu, T. Wang, and Q. Zhang, "A novel angle algorithm of polarization sensor for navigation," *IEEE Transactions on Instrumentation and Measurement*, vol. 58, no. 8, pp. 2791–2796, 2009.